A wake model for free-streamline flow theory

Part 2. Cavity flows past obstacles of arbitrary profile

By T. YAO-TSU WU AND D. P. WANG

Kármán Laboratory, California Institute of Technology

(Received 6 June 1963)

In Part 1 of this paper a free-streamline wake model was introduced to treat the fully and partially developed wake flow or cavity flow past an oblique flat plate. This theory is generalized here to investigate the cavity flow past an obstacle of arbitrary profile at an arbitrary cavitation number. Consideration is first given to the cavity flow past a polygonal obstacle whose wetted sides may be concave towards the flow and may also possess some gentle convex corners. The general case of curved walls is then obtained by a limiting process. The analysis in this general case leads to a set of two functional equations for which several methods of solution are developed and discussed.

As a few typical examples the analysis is carried out in detail for the specific cases of wedges, two-step wedges, flapped hydrofoils, and inclined circular arc plates. For these cases the present theory is found to be in good agreement with the experimental results available.

1. Introduction

The general theory of potential flows past curved obstacles with a free boundary formation has been long recognized as an interesting but difficult mathematical problem. The questions of construction, calculation, as well as existence and uniqueness have intrigued many outstanding hydrodynamicists and mathematicians alike. The celebrated work of Levi-Civita (1907) for the infinite cavity case has provided the basis for the general theory by introducing a convenient parametrization of the flow by which the solution is expressed in terms of an arbitrary analytic function in a half unit circle, and thereby removing the unknown free boundary from the question. Levi-Civita's representation has been further advanced by Villat (1911) who formulated the flow problem in terms of functional integral equations which have played a central role in the existence theory and the actual construction of the solution. Detailed discussions of these fundamental articles and the related developments can be found in the recent literature on this subject, for example, Gilbarg (1960), Birkhoff & Zarantonello (1957).

It has been noticed that perhaps the most complex and difficult problem of all is the actual computation of the solution. Some practical aspects of these difficulties have been discussed by Birkhoff & Zarantonello (chapter 9). This problem is largely unavoidable since for cavity flows past curved obstacles, even with infinite cavities, numerical methods seem to be the only means of obtaining

an accurate solution from the exact theory. While several finite-cavity flow models have also been considered together with the corresponding functional equations of Villat's type (see, e.g., Gilbarg 1960), the incorporation of these models only magnifies the complexities of the computation. One approximate method in common use is to make the continuous curvature equation discrete by a polynomial representation and to solve the resulting set of equations by direct iteration. However, this iteration has been shown to diverge for large values of a certain parameter M (which relates the scale of potential and that of the physical plane); for such cases a more elaborate averaged iteration has been introduced by Birkhoff, Goldstine & Zarantonello (1954). From our experience, the difficulties become particularly noticeable in the case of thin curved barriers held at small incidences to the flow since the total variation of the integrand in the functional equations increases rapidly with decreasing angle of attack. Unfortunately, this is also the case of considerable interest from the viewpoint of practical applications, such as cavitating hydrofoils and stalled airfoils. In short, it seems that so far none of the general iteration methods have been rigorously proved to converge, and theoretical estimates of error are still lacking.

The main objectives of this paper are twofold: (1) to develop an exact theory for the general case of arbitrary body profile and arbitrary cavitation number by adopting a rather simple wake model and by using a different parametrization, (2) to examine various numerical schemes which can be applied uniformly in the incidence angle and the cavitation number.

In part 1 of this paper (Wu 1962) a free-streamline wake model was introduced to treat the flow past an oblique flat plate with a fully or partially developed wake (or cavity) formation. According to this model the wake flow is approximately described in the large by an equivalent potential flow past the body with an infinitely long wake which consists of a near-wake of constant under-pressure and a far-wake trailing downstream. The pressure increases continuously back to its free-stream value along the far-wake boundary which is assumed to form a branch slit of an unknown shape in the hodograph plane.

This theory will now be generalized to evaluate the wake (or cavity) flow past an obstacle of arbitrary profile at arbitrary cavitation number. Consideration is first given to a polygonal obstacle whose wetted sides may be concave towards the flow and may also possess some gentle convex corners. The parametric plane of the flow is chosen to be in a half unit circle, with the circular arc corresponding to the constant pressure free boundary and the diameter to the wetted surface in such a way that this plane becomes the hodograph as the polygon is degenerated to a flat plate. The general case of curved walls is then deduced by a limiting process. The analysis in this general case leads to a set of two functional equations which are quite similar to Villat's equations. These equations immediately provide the exact solution of a wide class of 'inverse problems'. While the general direct problems are still difficult to solve exactly, the computation of the present theory is, however, not further complicated by non-vanishing cavitation numbers (aside from the determination of an additional scalar parameter). Several numerical methods for the general purpose have been developed here, some of which have already been applied with success.

In order to exhibit some salient features of cavity flows past curved obstacles, such as the effects of camber, cavitation number, incidence angle, and so forth, as well as to achieve a sound grasp of the convergence of various numerical schemes, the analysis and the subsequent computation have been carried out in detail for several typical examples: wedge, two-step wedge, hydrofoil with a flap, and inclined circular arc plate. The methods adopted have been found to converge in every case tried. Furthermore, in these cases the present theory is found to be in good agreement with the experimental results available.

2. Cavity flows and wake flows past a polygonal obstacle

We consider first the steady, plane, potential flow of an incompressible fluid past a polygonal obstacle with a wake or cavity formation in such a way that the N sides of the polygon are wetted and the flow is separated from fixed leading and trailing edges A and B, forming two free streamlines ACI and $BC'I$, as shown in the physical plane $z = x + iy$ of figure 1. The free stream at infinity is inclined at an angle α with the x-axis which may be chosen (but not necessarily) to coincide with the chord AB. Let $z_0 = z_A, z_1, z_2, \ldots, z_N = z_B$ be the vertices of the polygon; and let $(1+\epsilon_k)\pi$ be the exterior angle (on the cavity side) subtended by the consecutive sides at z_k, $k = 1, 2, \ldots, (N-1)$.

The polygonal wall may be concave towards the flow and may also possess some gentle convex corners so long as the resulting flow configuration provides a valid approximation of the actual physical flow. It is noted that the potential flow at such a convex corner, if not a stagnation point, must be singular there. Whether the flow is actually separated or not from such convex corners, however, should be investigated by including the relevant real fluid effects such as the viscous boundary layer at the wall, convection and diffusion of dissolved gases, as well as other properties of incipient cavitation. These real fluid effects are rather complicated and difficult to be taken into an accurate account; they will not be further discussed in this work. In the present formulation the flow around such convex corners may be regarded as an approximation to the actual case in which either the real fluid effects under the circumstances keep the flow from being separated or there exists only a small separated bubble with an immediate reattachment to the solid surface, so that no serious error results from neglecting such detailed local structure of the flow. To permit such gentle convex corners to remain wetted in the cavity flow is essential when we later generalize this analysis by a limiting process for obstacles of arbitrary profile. With this additional degree of freedom, ϵ_k is positive or negative according as the boundary at z_k is concave or convex towards the flow. It should be emphasized, nevertheless, that due caution must be exercised and the possibility of change in the basic flow pattern considered (for small enough α the flow in figure 1 may change the separation point from B to z_3, thus leaving z_3B inside the cavity).

Adopting the same notation as in Part 1, we have the complex potential $f(z) = \phi + i\psi$, and the complex velocity

$$w(z) = df/dz = u - iv = q\,e^{-i\theta}. \tag{1}$$

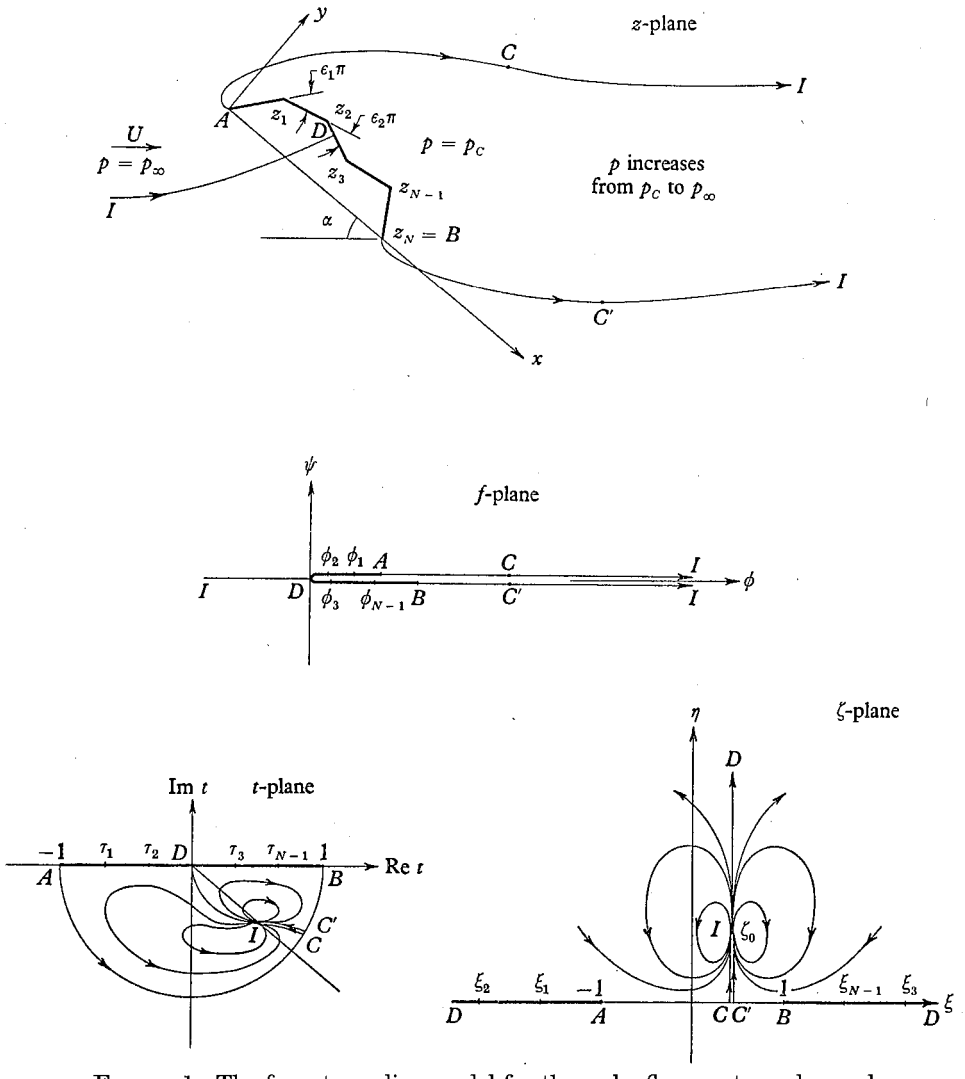

FIGURE 1. The free-streamline model for the wake flow past a polygonal obstacle and its conformal mapping planes.

The free stream has velocity U and incidence angle α, so

$$w = U e^{-i\alpha} \quad \text{at} \quad z = \infty. \tag{2}$$

The general description of the present wake flow model has been given in Part 1, which may be summarized here for the convenience of subsequent application. The part AC and BC' of the free streamlines form the lateral boundary of a near-wake of constant pressure

$$p = p_c < p_\infty \quad \text{on} \quad AC \quad \text{and} \quad BC', \tag{3}$$

p_∞ being the free-stream pressure. From this part onward p varies continually and monotonically from p_c to p_∞ along the far-wake boundary, CI and $C'I$. It is further assumed that

$$f_C = f_{C'}, \quad w_C = w_{C'}. \tag{4}$$

Moreover, the images of the free streamlines CI and $C'I$ are assumed to form a branch slit of undetermined shape in the w-plane (the hodograph-slit condition). The Bernoulli equation of the external flow is

$$p+\tfrac{1}{2}\rho q^2 = p_\infty+\tfrac{1}{2}\rho U^2 = p_c+\tfrac{1}{2}\rho q_c^2, \tag{5}$$

where q_c is the constant value of q along AC and BC'. With q_c normalized to unity, we have

$$q_c = 1, \quad U = (1+\sigma)^{-\frac{1}{2}}, \tag{6a}$$

where

$$\sigma = (p_\infty - p_c)/(\tfrac{1}{2}\rho U^2), \tag{6b}$$

σ being the wake under-pressure coefficient, or the cavitation number for cavity flows. Condition (3) is written for the case of full wake flow; for the partial wake flow case (see Part 1 for further details) the constant pressure portion BC' behind the trailing edge B then disappears.

For the present problem we introduce the ζ and t parameter planes by

$$f = \tfrac{1}{4}A(\zeta-\zeta_0)^{-1}(\zeta-\bar{\zeta}_0)^{-1}, \tag{7}$$

$$\zeta = \tfrac{1}{2}(t+t^{-1}), \tag{8}$$

where A is a positive real constant and the complex constant ζ_0 is the image point (yet undetermined) of $z=\infty$. The flow regions in the ζ and t-planes are shown in figure 1. The local conformal behaviour at C and C' requires that

$$df/d\zeta = O(|\zeta-\zeta_C|) \quad \text{as} \quad |\zeta-\zeta_C| \to 0,$$

from which it follows that

$$\zeta_C = \zeta_{C'} = \operatorname{Re}\zeta_0. \tag{9a}$$

Moreover, the line segments CI, $C'I$ and DI are seen from (7) to be straight lines parallel to the $\operatorname{Im}\zeta$-axis. The fully cavitating flow is again specified by the condition that the point C' falls downstream of the trailing edge B, or

$$\zeta_{C'} = \operatorname{Re}\zeta_0 \leqslant 1. \tag{9b}$$

When the numerical result gives $\operatorname{Re}\zeta_0 > 1$, the flow may be supposed to have undergone transition to become partially cavitating.

Equations (7) and (8) can be combined to give

$$f(t) = At^2[(t-t_0)(t-\bar{t}_0)(t-t_0^{-1})(t-\bar{t}_0^{-1})]^{-1}, \tag{10}$$

where t_0, from (8), is given by $t_0 = \zeta_0-(\zeta_0^2-1)^{\frac{1}{2}}$. The use of the variable t is suggested by the analysis of Part 1: here t plays the role of the variable w of the wake flow past an oblique flat plate (see Part 1) so that with $t \equiv w$, (10) provides the required solution of the flat-plate problem.

The solution of the present problem is seen to be best represented in the parametric form $f = f(t)$ and $w = w(t)$. We proceed now to determine the latter part $w = w(t)$. Let the points $\tau_1, \tau_2, \ldots, \tau_{N-1}$ on the real diameter of the t-plane $(-1 < \tau_1 < \tau_2 < \ldots < \tau_{N-1} < 1)$ correspond to the vertices $z_1, z_2, \ldots, z_{N-1}$ of the wall. We further let the stagnation point D, at which $w = 0$, be chosen at $t = 0$. Now, as the point z moves along the polygonal boundary from A to B, $\operatorname{Im}(\log w) = \arg w$ remains constant on every straight segment, jumps by $(\epsilon_k \pi)$

as z moves across the vertex z_k, and jumps by π as z goes over the stagnation point. Furthermore, along AC and BC', where $|t| = 1$, we have

$$\mathrm{Re}\,(\log w) = \log q_c = 0.$$

From these two conditions one sees by inspection that

$$w(t) = e^{-i\beta_0} t \prod_{k=1}^{N-1} \left(\frac{t-\tau_k}{\tau_k t - 1}\right)^{\epsilon_k}, \tag{11}$$

where β_0 is the angle made by the leading segment with the x-axis, positive in the counterclockwise sense. It is obvious that the above w satisfies the conditions on $\arg w$ over the solid boundary. Furthermore, with $-1 < \tau < 1$ and δ real, the conformal transformation

$$T = \exp(i\delta)\,(t-\tau)/(\tau t - 1) \tag{11a}$$

maps the circle $|t| = 1$ on $|T| = 1$, and we have $|T| < 1$ when $|t| < 1$. This establishes the solution (11). In particular, when β_0 and all ϵ_k vanish, w and t become identical, leaving (10) as the known solution of the flat-plate problem (see Part 1).

Equations (10) and (11) give the parametric solution $f = f(t)$, $w = w(t)$. The solution is completed when the physical z-plane is determined from

$$z(t) = \int_{-1}^{t} \frac{1}{w(t)} \frac{df}{dt} dt. \tag{12}$$

The above integral cannot in general be integrated in a closed form.

It is noted that the solution given by (10), (11) and (12) contains $(N+1)$ parameters $A, t_0, \tau_1, \ldots, \tau_{N-1}$ ($N+2$ real parameters as only t_0 is complex) which can be determined by the following consideration. First, at $z = \infty$, or $t = t_0$, application of condition (2) to (11) yields

$$U e^{i(\beta_0 - \alpha)} = t_0 \prod_{k=1}^{N-1} \left(\frac{t_0 - \tau_k}{\tau_k t_0 - 1}\right)^{\epsilon_k}. \tag{13}$$

The region of $|t_0|$ for the particular case of all $\epsilon_k > 0$ can be seen from (13), (11a) to be

$$U < |t_0| < 1, \quad \text{if all} \quad \epsilon_k > 0. \tag{13a}$$

Furthermore, the length of the kth segment is

$$l_k \equiv |z_k - z_{k-1}| = \int_{\tau_{k-1}}^{\tau_k} \frac{1}{|w|} \left|\frac{df}{dt}\right| dt \quad (k = 1, 2, \ldots, N). \tag{14}$$

Finally, we also have

$$z_B - z_A = \int_{-1}^{1} \frac{1}{w} \frac{df}{dt} dt = l e^{i\alpha_c}, \tag{15}$$

where l is the chord length and α_c the inclination of the chord. Equations (13) and (14) form $(N+1)$ equations, which are in general non-linear and transcendental, for the $(N+1)$ parameters $A, t_0, \tau_1, \ldots, \tau_{N-1}$. For further discussion on the determination of these parameters, we distinguish between the following two cases.

3. The direct and inverse problem; numerical iteration methods

The original physical or direct problem is specified with prescribed geometry (all l_k and ϵ_k given) and flow configuration (α and the cavitation number σ or U given), there being a total of $(2N+1)$ direct physical parameters,

$$P(\alpha;\, \sigma;\, l_1, \ldots, l_N;\, \epsilon_1, \ldots, \epsilon_{N-1}). \tag{16a}$$

A wake flow past a N-sided polygon can therefore be represented by a point P in a $(2N+1)$-dimensional space with the above co-ordinates. The region of these co-ordinates permissible for our physical problem may be described as

$$R(|\alpha| < \tfrac{1}{2}\pi;\, \sigma > 0;\, l_k > 0;\, \delta_k < \epsilon_k < 1), \tag{16b}$$

where δ_k, the lower limit of ϵ_k, may be zero or may assume some small negative value (in order to render a valid approximation of the actual motion, as explained earlier). Aside from this qualifying condition, no definite lower bound of the negative value can be stated in general for δ_k. If, however,

$$\delta_k \geqslant 0,\ k = 1, 2 \ldots, N-1,$$

then the wetted surface is concave to the flow.

On the other hand, our solution given by (10)–(14) also defines a wake flow past a N-sided polygon which can be represented by $(2N+1)$ 'inverse flow' parameters

$$P'(A;\, t_0\,(\text{complex});\, \tau_1, \ldots, \tau_{N-1};\, \epsilon_1, \ldots, \epsilon_{N-1}), \tag{17a}$$

with the corresponding region

$$R'(A > 0;\, |t_0| < 1,\, -\pi < \arg t_0 < 0;\, -1 < \tau_1 < \ldots < \tau_{N-1} < 1;\, \delta_k < \epsilon_k < 1). \tag{17b}$$

For the more restricted case of $\delta_k = 0$ in (16*b*) and (17*b*) the corresponding region will be denoted by R_* and R'_*. For definiteness some statement in the sequel will be made on the basis of the region R_* and R'_* since the relaxed case when ϵ_k may assume small negative values must eventually depend on experimental verification.

Let us consider the inverse problem by choosing a point P' within the region R'_*. Then, since $|\tau_k| < 1$ and $|t_0| < 1$, it follows from (13) that

$$U = |t_0| \prod_{k=1}^{N-1} \left| \frac{t_0 - \tau_k}{\tau_k t_0 - 1} \right|^{\epsilon_k} < 1, \tag{18a}$$

so that $\sigma = (U^{-2} - 1) > 0$. Equating the argument of (13), we obtain the incidence $(\alpha - \beta_0)$ of the leading segment

$$\alpha - \beta_0 = -\arg t_0 + \sum_{k=1}^{N-1} \epsilon_k [\arg(\tau_k t_0 - 1) - \arg(t_0 - \tau_k)]. \tag{18b}$$

The entire configuration is then fixed (up to a common scale factor A), with the length l_k of every segment given by (14). Therefore, to each P' in R'_* there corresponds a single P in R_*. In this sense we may assert that the mathematical solution of an inverse problem *exists* and is *unique*.

In the direct problem with prescribed P, there are $(N+1)$ unknown parameters $A; t_0; \tau_1, \ldots, \tau_{N-1}$, which have to be determined from the $(N+1)$ transcendental equations (13) and (14). These equations are in general very difficult to solve directly. The existence and uniqueness consideration for the original physical problem is to establish the converse statement that to each point P there corresponds one and only one P', or in other words that the $(N+1)$ non-linear equations (13) and (14) possess a unique solution of the $(N+1)$ unknown parameters for any prescribed values of the physical parameters in P. The problem of existence and uniqueness may be treated by adopting the idea of 'local uniqueness' as used by Weinstein (1924, 1927, 1929), and Leray (1934, 1935) for similar problems in the theory of free-boundary flows. The details of such considerations, however, will not be pursued further in this work.

The above consideration of the inverse problem provides a basis of constructing approximate methods for the direct physical problem. We have essentially established two such methods: (i) an integral iteration scheme, and (ii) a differential perturbation approximation, both depending on a known basic flow as the reference. The difference between the actual flow and the basic flow need not be very small for the first method as long as the iteration converges, whereas this difference is assumed small for the second method to be effective. The integral iteration for polygonal obstacles is best presented as a special case of the general method for curved profiles; this is done in §5.1. We present below the differential perturbation method as it may also bear some interest regarding the problem of existence and uniqueness.

Suppose that a basic flow $P(\alpha; \sigma; l_1, \ldots, l_N; \epsilon_1, \ldots, \epsilon_{N-1})$ is given by (13) and (14) with prescribed parameters $P'(A; t_0; \tau_1, \ldots, \tau_{N-1}; \epsilon_1, \ldots, \epsilon_{N-1})$. Let these parameters be given variations δA, δV, $\delta\alpha_0$, $\delta\tau_k$, $\delta\epsilon_k$, where $t_0 = V e^{-i\alpha_0}$. Then the corresponding variations of the physical parameters are given by

$$\delta l_j = \frac{\partial l_j}{\partial A}\delta A + \frac{\partial l_j}{\partial V}\delta V + \frac{\partial l_j}{\partial \alpha_0}\delta\alpha_0 + \sum_{k=1}^{N-1}\left(\frac{\partial l_j}{\partial \tau_k}\delta\tau_k + \frac{\partial l_j}{\partial \epsilon_k}\delta\epsilon_k\right), \tag{19a}$$

$$\delta\epsilon_k = \delta\epsilon_k \quad (k = 1, 2, \ldots, N-1), \tag{19b}$$

$$\delta U = \frac{\partial U}{\partial V}\delta V + \frac{\partial U}{\partial \alpha_0}\delta\alpha_0 + \sum_{k=1}^{N-1}\left(\frac{\partial U}{\partial \tau_k}\delta\tau_k + \frac{\partial U}{\partial \epsilon_k}\delta\epsilon_k\right), \tag{19c}$$

$$\delta\alpha = \frac{\partial \alpha}{\partial V}\delta V + \frac{\partial \alpha}{\partial \alpha_0}\delta\alpha_0 + \sum_{k=1}^{N-1}\left(\frac{\partial \alpha}{\partial \tau_k}\delta\tau_k + \frac{\partial \alpha}{\partial \epsilon_k}\delta\epsilon_k\right), \tag{19d}$$

where in (19 a), $j = 1, 2, \ldots, N$. In (19 c) U may be replaced by σ since $\sigma = (U^{-2} - 1)$. The coefficients of the above set of $(2N+1)$ equations can be readily deduced by differentiation of (13) and (14); their explicit expressions will not be given here.

Conversely, if a physical flow is given by $P_*(\alpha; \sigma; l_k + \delta l_k; \epsilon_k + \delta\epsilon_k)$ which in turn may be regarded as a variation of the basic flow at fixed α and σ, then the corresponding variation of the inverse parameters can be obtained by solving the $(2N+1)$ linear equations (19) with the known quantities δl_k, $\delta\epsilon_k$, $\delta U = 0$, $\delta\alpha = 0$, provided that the Jacobian

$$\partial(\alpha; \sigma; l_1, \ldots, l_N; \epsilon_1, \ldots, \epsilon_{N-1})/\partial(A; V; \alpha_0; \tau_1, \ldots, \tau_{N-1}; \epsilon_1, \ldots, \epsilon_{N-1}) \tag{20}$$

is non-vanishing. The last statement would also imply existence and uniqueness.

The above perturbation theory can be applied to construct an iteration scheme as follows. We combine the so determined variation $(\delta A, \delta V, \delta\alpha_0, \delta\tau_k, \delta\epsilon_k)$ with the original reference flow to provide a new reference flow $P_1'(A+\delta A, V+\delta V, \alpha_0+\delta\alpha_0, \tau_k+\delta\tau_k, \epsilon_k+\delta\epsilon_k)$ which, by using (13) and (14) as an inverse problem, provides in turn a new physical flow $P_1(\alpha^{(1)}, \sigma^{(1)}, l_k^{(1)}, \epsilon_k^{(1)})$. By comparison of P_1 with the given flow P_* a set of new variations $(\delta\alpha, \delta\sigma, \delta l_k, \delta\epsilon_k)$ of the physical parameters is obtained, thus enabling one to proceed by repeating the process iteratively over and over again. Needless to say, the success of this iteration process depends on how fast the set $P_n(\alpha^{(n)}, \sigma^{(n)}, l_k^{(n)}, \epsilon_k^{(n)})$ converges to the prescribed physical flow.

It may be remarked that the first reference flow need not have the same number N of faces. For example, when all the ϵ_k's are small, the cavity flow past the flat plate spanning along the chord AB can be used as the basic flow, in which case the complex velocity w of the basic flow coincides with t, and $\tau_1, \ldots, \tau_{N-1}$ of the basic flow become the image in the t-plane of those points on the flat plate which are at the same length apart as the vertices of the given polygon (in other words, δl_k are all chosen to be zero for the first iteration).

4. Obstacles with arbitrary profile; the functional equations

The preceding results can be readily extended to contain the general case when the obstacle has an arbitrary profile. This generalization is quite straightforward for the case of *fixed detachment* when the detachment points (in general at sharp corners) are assumed known. The theory can also be applied to the problem of *smooth detachment*, when the detachment points (at a smooth surface, for example) cannot be prescribed in advance, provided some additional appropriate conditions are imposed for their determination. The condition generally adopted for this type of problem is based on Villat's criterion (1914) which requires the curvature of the free streamline to be finite at the point of smooth detachment.

Thus we presume that the free streamlines become detached from the body at points A and B (with either fixed or smooth detachment) to form a wake or cavity, as depicted in figure 2. The wetted surface of the obstacle may be expressed parametrically as

$$x = x(s), \quad y = y(s) \quad \text{for} \quad 0 \leqslant s \leqslant S, \tag{21a}$$

where S is the total arc length of the wetted surface. These functions and their first derivatives may be assumed Hölder continuous in s for $0 \leqslant s \leqslant S$. The inclination angle of the body surface with the x-axis is

$$\beta(s) = \tan^{-1}\left(\frac{dy}{ds}\Big/\frac{dx}{ds}\right) \quad (0 \leqslant s \leqslant S). \tag{21b}$$

Here the variation of β need not be limited to be small as long as the resulting flow is supported by physical observations. The maximum variation of β, defined as the difference between the maximum and minimum value of β, may be taken to be less than π and may be considerably smaller in ordinary cases of practical applications.

Let us consider a limiting process by which the number N of the polygonal faces increases beyond all bounds, the face lengths l_k all tend to zero, and the turning angles ϵ_k all become vanishingly small except possibly at a finite number of isolated points where the obstacle has sharp corners. In the limit as $N \to \infty$ and $|\epsilon_k| \to 0$, we may rewrite (11) as

$$w = e^{-i\beta_0} t \exp\left\{\sum_{k=1}^{N-1} \epsilon_k \log\left(\frac{t-\tau_k}{\tau_k t - 1}\right)\right\},$$

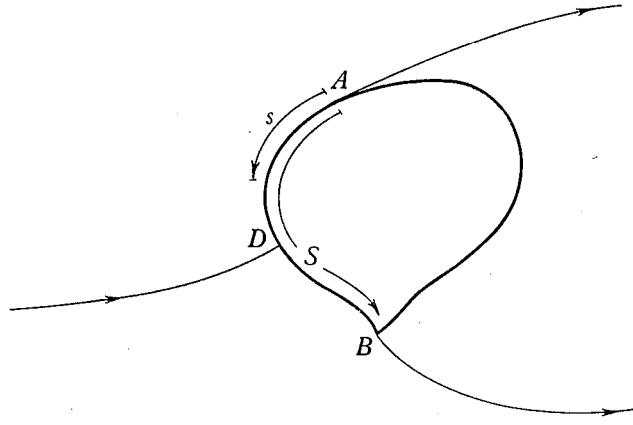

FIGURE 2. Free-streamlines with fixed and smooth detachment from a solid boundary.

and then replace the summation by an integration with respect to the continuous variable τ, substituting $\epsilon_k \pi$ by $(-d\beta)$ where $\beta(\tau)$ is the inclination angle of the body surface at the point $t = \tau$. (The negative sign of $(-d\beta)$ is taken on account of the original convention of the positive sense of ϵ_k.) We therefore obtain

$$w = e^{-i\beta_0} t \exp\left\{-\frac{1}{\pi}\int_{-1}^{1} \log\left(\frac{t-\tau}{\tau t - 1}\right)\frac{d\beta}{d\tau}\,d\tau\right\}, \tag{22}$$

where clearly $\beta_0 = \beta(-1)$. It may be noted that this result includes the special case (11) for polygonal bodies when we take

$$\frac{d\beta}{d\tau} = -\sum_{k=1}^{N-1} (\epsilon_k \pi)\,\delta(\tau - \tau_k),$$

$\delta(\tau - \tau_k)$ being the Dirac delta function. Integrating the integral in (22) by parts, we find that the contribution at the lower limit $\tau = -1$ (where $\beta = \beta_0$ and $\log[(t-\tau)/(t\tau - 1)] = i\pi$) cancels the factor $\exp(-i\beta_0)$, giving

$$w(t) = t \exp\left\{-\frac{(1-t^2)}{\pi}\int_{-1}^{1} \frac{\beta(\tau)\,d\tau}{(\tau - t)(\tau t - 1)}\right\}. \tag{23}$$

The exact solution is therefore expressed parametrically as $f = f(t)$, $w = w(t)$, with $f(t)$ given by (10) and $w(t)$ by (22) or (23). As a remark, the above solution $w(t)$ can also be obtained directly by the method of functional theory (see Appendix).

The form (22) is based on the curvature whereas (23), on the inclination of the body surface. In fact, the curvature of a bounding streamline, defined by $\kappa = d\theta/ds$ (s being the arc length along the streamline), can be written

$$\kappa = \frac{d\theta}{ds} = \frac{\partial\theta}{\partial\phi}\frac{\partial\phi}{\partial s} = \mathrm{Re}\left(q\frac{d\omega}{df}\right) = \mathrm{Re}\left(e^{\lambda}\frac{d\omega}{df}\right), \tag{24a}$$

where

$$\omega = i\log w = \theta + i\lambda. \tag{24b}$$

Hence on the body, $\theta = \beta$ (or they may differ by at most a constant),

$$\kappa_S = q\frac{d\beta}{d\phi} = e^{\lambda(t)}\frac{d\beta}{dt}\Big/\frac{df}{dt} \quad (-1 < t < 1); \tag{25a}$$

and on the cavity boundary where $\lambda = 0$,

$$\kappa_C = \frac{d\omega}{df} = \frac{d\omega}{dt}\Big/\frac{df}{dt} \quad (t = e^{-i\chi},\ 0 < \chi < \pi). \tag{25b}$$

Finally, the physical z-plane is again determined by (12), except now $w(t)$ is given by (22) or (23). In particular, on the body (t real),

$$z(t) = \int_{-1}^{t} e^{i\beta(t)}\exp\left\{\frac{(1-t^2)}{\pi}\,{\overset{*}{\int}}_{-1}^{1}\frac{\beta(\tau)\,d\tau}{(\tau-t)(\tau t-1)}\right\}\frac{df}{dt}\frac{dt}{t}, \tag{26a}$$

in which * above the integral sign signifies the Cauchy principal value. Since for real t,

$${\overset{*}{\int}}_{-1}^{1}\frac{d\tau}{(\tau-t)(\tau t-1)} = 0,$$

we may also write for the points on the solid surface, or for t real,

$$z(t) = \int_{-1}^{t} e^{i\beta(t)}\exp\left\{\frac{(1-t^2)}{\pi}\int_{-1}^{1}\frac{\beta(\tau)-\beta(t)}{(\tau-t)(\tau t-1)}\,d\tau\right\}\frac{df}{dt}\frac{dt}{t}. \tag{26b}$$

Since $dz = (ds)\,e^{i\beta}$, it therefore follows from (26b) that the arc length $s(t)$ along the body surface, measured from the leading edge A, is

$$s(t) = \int_{-1}^{t}\exp\left\{\frac{(1-t^2)}{\pi}\int_{-1}^{1}\frac{\beta(\tau)-\beta(t)}{(\tau-t)(\tau t-1)}\,d\tau\right\}\frac{df}{dt}\frac{dt}{t}. \tag{27}$$

The above formal solution contains two arbitrary parameters A and t_0, and an arbitrary real function $\beta(t)$. They are governed by the following conditions. First, application of condition (2) to (23) yields

$$U e^{-i\alpha} = t_0\exp\left\{-\frac{(1-t_0^2)}{\pi}\,{\overset{*}{\int}}_{-1}^{1}\frac{\beta(\tau)\,d\tau}{(\tau-t_0)(\tau t_0-1)}\right\}. \tag{28}$$

Next, let us consider the boundary condition on the solid surface. In the case of fixed detachment, the angle β is a given function of s (see (21)). However, $s(t)$ and hence $\beta(t) = \beta(s(t))$, which appear in (27) and (28), are not known *a priori*. Thus the right-hand side of (27) and (28) may be regarded as two integral operators $\mathscr{I}_1[s(t), \beta(s); t_0]$ and $\mathscr{I}_2[s(t), \beta(s); t_0]$ depending on $s(t), \beta(s)$ and the parameter t_0,

which provide the functional transformations of $s(t)$ into the left-hand side member of (27) and (28), or symbolically,

$$s(t)/A = \mathscr{J}_1[s(t), \beta(s(t)); t_0], \tag{29}$$

$$U e^{-i\alpha} = \mathscr{J}_2[s(t), \beta(s(t)); t_0], \tag{30}$$

the right-hand sides of these equations being independent of the parameter A. Equations (29) and (30) are a set of functional equations for the unknowns $s(t; t_0)$, $\beta(t)$ and t_0. Finally, the parameter A is fixed by the physical scale of the total arc length

$$s(1) = S. \tag{31}$$

For the problem of smooth detachment, each smooth-separation point becomes an additional unknown for which another condition must be imposed for its determination. We may adopt the finite curvature condition that

$$\frac{d\omega}{dt} = 0 \quad \text{at} \quad t = \mp 1, \tag{32a}$$

where $\omega = i \log w$, and where $t = -1$ (or 1) is applicable when the smooth detachment occurs at A (or B). This can be seen as follows. From the local conformal behaviour of $f(t)$ at $t = \mp 1$ it is obvious that df/dt vanishes like $(t \pm 1)$ as $|t \pm 1| \to 0$. Therefore the curvature of the free streamline ($\kappa_c = d\omega/df$, see (25b)) will be infinite at the detachment unless $d\omega/dt$ also vanishes there. In the latter case it follows from Villat's alternative (Villat 1914) that the curvature of the free streamline at detachment coincides with that of the body. By using (23), condition (32a) can further be written

$$\lim_{t \to \pm 1} \left\{ \frac{1}{t} + \frac{1}{\pi} \frac{d}{dt} \int_{-1}^{1} \left(\frac{1}{\tau - t} - \frac{1}{\tau - t^{-1}} \right) \beta(\tau) \, d\tau \right\} = 0, \tag{32b}$$

which must be used together with the previous conditions to determine $\beta(s(t))$, t_0 and A.

The above considerations provide a means of constructing inverse and approximate solutions of the cavity problem. For the inverse problem we begin with an adequate choice of t_0 and the function $\beta(t)$, then α and U (or σ) can be calculated directly from (28), and the geometrical configuration by quadrature from (26). Again, the body profile varies for different α and σ. The exact solution of an appropriate inverse problem can also be used as the reference flow for approximate solutions of the original physical problem.

5. Numerical iteration and approximate methods

The general profile of the curved obstacle may admit $(N-1)$ isolated sharp corners across each of which (say at z_k) the inclination β jumps by $(-\epsilon_k \pi)$ so that we may write

$$\beta(s) = -\sum_{k=1}^{N-1} (\epsilon_k \pi) H(s - s_k) + \gamma(s), \tag{33}$$

where s_k is the arc length from A to z_k, and H is the Heaviside step function. Clearly $\gamma(s)$ is continuous everywhere on the wetted surface. We present in the following two numerical schemes, the first one being entirely general, whereas the second is characteristic for a particular category of profiles.

5.1. *An integral iteration method*

The following integral iteration method has been developed for the general purpose and has been found to be relatively simple and straightforward to apply. Suppose there exists a known basic flow referred to which the flow in question may be regarded as a (not necessarily small) perturbation. For convenience the basic flow may be chosen as simple as practical; for example, one may chose an inclined flat plate if $\beta(s)$ is everywhere small, or a two-sided wedge spanning the same end points A and B if $\beta(s)$ is moderate or large. The exact solution of the basic flow will be denoted by

$$\beta = \beta^{(0)}(s), \quad s = s^{(0)}(t; t^{(0)}), \quad t_0^{(0)}, \quad A^{(0)}. \tag{34}$$

The function $\beta^{(0)}(s)$ is of course different from $\beta(s)$ of (33).

Equations (27) and (28) may be rewritten for the iteration scheme as

$$\frac{1}{A^{(n)}} s^{(n)}(t; t_0^{(n)}) = \int_{-1}^{t} \mathscr{E}[\beta(s^{(n-1)}(t; t_0^{(n-1)}))] \frac{d}{dt}\left[\frac{f(t; t_0^{(n-1)})}{A^{(n-1)}}\right] \frac{dt}{t}, \tag{35}$$

$$t_0^{(n)} = U e^{-i\alpha} \mathscr{F}[\beta(s^{(n-1)}(t; t_0^{(n-1)}))], \tag{36}$$

for $n = 1, 2, 3, \ldots$, where

$$\mathscr{E}[\beta(s(t; t_0))] \equiv \exp\left\{\frac{(1-t^2)}{\pi} \int_{-1}^{1} \frac{\beta(\tau) - \beta(t)}{(\tau - t)(\tau t - 1)} d\tau\right\}, \tag{37}$$

$$\mathscr{F}[\beta(s(t; t_0))] \equiv \exp\left\{\frac{(1-t_0^2)}{\pi} \int_{-1}^{1} \frac{\beta(\tau)\, d\tau}{(\tau - t_0)(\tau t_0 - 1)}\right\}. \tag{38}$$

Here $\beta(s^{(n)}(t))$ assumes the corresponding value of the prescribed $\beta(s)$ with $s = s^{(n)}(t)$ for $n = 0, 1, 2, \ldots, s^{(0)}(t)$ being provided by the basic flow. Other than this role, the inclination $\beta^{(0)}(s)$ of the basic flow never enters the iteration calculation explicitly. Finally, the physical scale factor $A^{(n)}$ of each n will be so chosen that

$$s^{(n)}(1) = S \quad \text{for} \quad n = 0, 1, 2, \ldots. \tag{39}$$

This condition ensures that the total arc length of the wetted surface in each iteration, including the basic flow, remains fixed (see condition (31)) so that the original boundary condition of the prescribed $\beta(s)$ can be applied in the entire interval $0 < s < S$. When the set of values $\{t_0^{(n)}\}$ and functions $\{s^{(n)}(t)\}$ tend to definite limits as $n \to \infty$, then this iteration converges to the required solution. In numerical work, estimates of $|s^{(n+1)}/s^{(n)} - 1|$ and $|t_0^{(n+1)}/t_0^{(n)} - 1|$ provide a good indication of the rate of convergence.

In the problem of smooth detachment one also has to apply the same iteration procedure to the additional condition (32*b*), use of which must yield convergent values of the detachment points if the solution is to be meaningful.

It should be pointed out here that this iteration method is universal so long as the integral operations involved can be carried out and the process is convergent. It therefore includes the special case of step-jump β for polygonal obstacles.

5.2. *Polynomial representation of $\beta(t)$*

Let us consider again the general case (33). While the determination of $\beta(t)$ is generally complicated, the values of β are nevertheless prescribed for the fixed

detachment points A and B, $\beta(-1) = \beta_A$, $\beta(1) = \beta_B$, say. Hence from (33) γ is also known at $t = \pm 1$, namely

$$\gamma_A = \gamma(-1) = \beta_A, \quad \gamma_B = \gamma(1) = \beta_B + \pi \sum_{k=1}^{N-1} \epsilon_k. \tag{40}$$

We may next expand the continuous function $\gamma(t)$ into a power series

$$\gamma(t) = \gamma_A \frac{1-t}{2} + \gamma_B \frac{1+t}{2} + \sum_{m=1}^{\infty} \sum_{n=1}^{\infty} \gamma_{mn} \left(\frac{1-t}{2}\right)^m \left(\frac{1+t}{2}\right)^n, \tag{41}$$

which satisfies condition (40) and converges uniformly and absolutely for $-1 < t < 1$. Furthermore, it is noted from (25) that the curvature of the solid surface near the detachment points is

$$\lim_{t \to \pm |1-0|} \kappa_S(t) = \lim_{t \to \pm 1} e^{\lambda(t)} \frac{d\beta/dt}{df/dt} = \lim_{t \to \pm 1} \frac{d\beta/dt}{df/dt}. \tag{42}$$

But it has already been noted that (df/dt) vanishes like $(1 \pm t)$ as $|1 \pm t| \to 0$. Therefore, as long as the curvature of the wetted surface is finite at the detachment, regardless of whether the detachment is fixed or smooth, the following two conditions,

$$\frac{d\beta}{dt} = \frac{d\gamma}{dt} = O(1 \pm t) \quad \text{as} \quad |1 \pm t| \to 0, \tag{43a}$$

must be satisfied, which, when applied to (41), yield

$$\gamma_B - \gamma_A = \sum_{n=1}^{\infty} \gamma_{1n} = -\sum_{m=1}^{\infty} \gamma_{m1}. \tag{43b}$$

Actually we can carry out the limit in (42) and apply the known curvature conditions at the detachment points; the result will however be omitted here.

An approximate method is obtained by taking a truncated series in (41) with M terms in m and N terms in n. For simplicity we shall describe this method for the special case of no sharp corners, and hence $\beta(s) = \gamma(s)$. Substituting this polynomial in (27) and (28), we obtain

$$s(t) = \int_{-1}^{t} \left(\frac{1+t}{1-t}\right)^{(\gamma_A - \gamma_B)(1-t^2)/2\pi t} \exp\left\{\frac{(1-t^2)}{\pi} \int_{-1}^{1} \frac{\gamma_{MN}(\tau) - \gamma_{MN}(t)}{(\tau - t)(\tau t - 1)} d\tau\right\} \frac{df}{dt} \frac{dt}{t}, \tag{44}$$

$$U e^{-i\alpha} = t_0 \left(\frac{t_0 - 1}{t_0 + 1}\right)^{(\gamma_A - \gamma_B)(1-t_0^2)/2\pi t_0} \times \exp\left\{-i\left(\frac{\gamma_A + \gamma_B}{2} + \frac{\gamma_B - \gamma_A}{2t_0}\right) - \frac{(1-t_0^2)}{\pi} \int_{-1}^{1} \frac{\gamma_{MN}(\tau)\, d\tau}{(\tau - t_0)(\tau t_0 - 1)}\right\}, \tag{45}$$

where

$$\gamma_{MN}(t) = \sum_{m=1}^{M} \sum_{n=1}^{N} \gamma_{mn} \left(\frac{1-t}{2}\right)^m \left(\frac{1+t}{2}\right)^n. \tag{46}$$

In addition to conditions (44), (45), we have of course conditions (43b), (31) and (32a) (the last one being for the smooth detachment case).

In case the change of the surface inclination is sufficiently smooth over the entire surface, especially near the points A and B, one may regard

$$\gamma^{(0)}(t) = (\gamma - \gamma_{MN})$$

as the reference flow and derive a linear problem for the coefficients γ_{mn}. An appropriate number of points on the real t-axis may be chosen for application of condition (44).

6. Lift and drag

The complex force $F = X + iY$ is seen to be

$$F = i\int_A^B (p-p_c)\,dz = \tfrac{1}{2}i\rho\int_{CABC'} (1-w\bar{w})\,dz = -\tfrac{1}{2}i\rho\oint_\Gamma (1-w\bar{w})\frac{dz}{dt}\,dt, \quad (47)$$

where the contour Γ is $C'BAC$. The first term of the last integral becomes

$$F_1 = -\tfrac{1}{2}i\rho\oint_\Gamma \frac{1}{w}\frac{df}{dt}\,dt = \tfrac{1}{2}i\rho\oint_\Gamma f\frac{d}{dt}\left(\frac{1}{w}\right)dt$$

by integration by parts; and the complex conjugate of the second integral is

$$\bar{F}_2 = \tfrac{1}{2}i\rho\int_{CABC'} w\bar{w}\,d\bar{z} = \tfrac{1}{2}i\rho\int_{CABC'} w\,df = \tfrac{1}{2}i\rho\oint_\Gamma f\frac{dw}{dt}\,dt.$$

Now the integrands of the last two integrals are analytic and regular everywhere inside the contour Γ except at the simple pole $t = t_0$. Since as $t \to t_0$

$$f(t) = \frac{B}{t-t_0} + O(1), \quad B = \frac{At_0^3\bar{t}_0}{(t_0-\bar{t}_0)(t_0^2-1)(t_0\bar{t}_0-1)}, \quad (48)$$

we obtain by the theorem of residues

$$F = F_1 + F_2 = -\pi\rho\left\{B\left[\frac{d}{dt}\left(\frac{1}{w}\right)\right]_{t=t_0} + \bar{B}\overline{\left[\left(\frac{dw}{dt}\right)_{t=t_0}\right]}\right\},$$

$$= \pi\rho e^{i\alpha}\left\{\frac{B}{U}\left(\frac{d\log w}{dt}\right)_{t=t_0} - \bar{B}U\overline{\left(\frac{d\log w}{dt}\right)_{t=t_0}}\right\}, \quad (49)$$

by using (2). Finally, the lift L and drag D are given by

$$D + iL = Fe^{-i\alpha} = \pi\rho\left\{\frac{B}{U}G(t_0) - U\overline{BG(t_0)}\right\}, \quad (50)$$

where $G(t) = d\log w/dt$, and hence for the polygonal obstacles

$$G(t) = \frac{1}{t} + \sum_{k=1}^{N-1} \epsilon_k \frac{1-\tau_k^2}{(t-\tau_k)(1-\tau_k t)}, \quad (50a)$$

and in general

$$G(t) = \frac{1}{t} + \frac{1}{\pi}\int_{-1}^{1}\left[\frac{1}{(\tau-t)^2} + \frac{1}{(\tau t-1)^2}\right]\beta(\tau)\,d\tau. \quad (50b)$$

7. Some basic features of the free streamlines

The shape of the free streamlines AC and BC' will now be determined. On the boundary AC and BC' of the near-wake,

$$t = e^{-i\chi} \quad (0 < \chi < \pi), \quad (51)$$

which corresponds to $\zeta = \xi = \cos\chi$. Then from (23) and (24b)

$$\omega = i\log w = (\cos^{-1}\xi) + \frac{2}{\pi}(1-\xi^2)^{\frac{1}{2}}\int_{-1}^{1}\frac{\beta(\tau)\,d\tau}{\tau^2 - 2\xi\tau + 1} \quad (|\xi| < 1). \quad (52)$$

Let the image point of $z = \infty$ be

$$t_0 = V e^{-i\alpha_0}, \quad \text{with} \quad 0 < V < 1, \quad 0 < \alpha_0 < \pi, \tag{53a}$$

or

$$\zeta_0 = \xi_0 + i\eta_0, \quad \xi_0 = \frac{1}{2}\left(\frac{1}{V} + V\right)\cos\alpha_0, \quad \eta_0 = \frac{1}{2}\left(\frac{1}{V} - V\right)\sin\alpha_0, \tag{53b}$$

with $|\xi_0| < 1$ for the fully developed wake flows. Then on AC and BC',

$$f = \tfrac{1}{4}A[(\xi - \xi_0)^2 + \eta_0^2]^{-1}. \tag{54}$$

The curvature of AC and BC', by (25b), is $\kappa_c = d\omega/df$, or

$$\kappa_c = \frac{2}{A}\frac{[(\xi-\xi_0)^2+\eta_0^2]^2}{(\xi-\xi_0)}\left\{(1-\xi^2)^{-\frac{1}{2}} - \frac{2}{\pi}\frac{d}{d\xi}\int_{-1}^{1}\frac{(1-\xi^2)^{\frac{1}{2}}\beta(\tau)\,d\tau}{\tau^2 - 2\xi\tau + 1}\right\}. \tag{55}$$

Thus the curvature of AC and BC' is in general singular at A, B, C and C'. The singular behaviour of the curvature at C and C', or at $\zeta = \xi_0$, is an intrinsic feature of this wake model.

A parametric representation of the free boundary AC and BC' can be obtained from

$$z(\xi) - z_A = \int_{-1}^{\xi}\frac{1}{w}\frac{df}{d\xi}d\xi = \frac{A}{2}\int_{-1}^{\xi} e^{i\omega(\xi)}\frac{(\xi_0-\xi)\,d\xi}{[(\xi_0-\xi)^2+\eta_0^2]^2} \quad (-1 < \xi < \xi_0), \tag{56a}$$

$$z(\xi) - z_B = \int_{1}^{\xi}\frac{1}{w}\frac{df}{d\xi}d\xi = \frac{A}{2}\int_{\xi}^{1} e^{i\omega(\xi)}\frac{(\xi-\xi_0)\,d\xi}{[(\xi-\xi_0)^2+\eta_0^2]^2} \quad (\xi_0 < \xi < 1), \tag{56b}$$

where $\omega(\xi)$ is given by (52).

8. Examples

In the preceding sections several numerical methods have been developed for the general purpose of evaluating the direct problems. In order to exhibit the important physical effects of cavity flows past curved bodies and at the same time to carry out these numerical schemes, we consider in the following a few typical examples: (A) symmetric wedges, (B) two-step wedges, (C) flat plate with a flap, (D) inclined circular arc. Case (A) contains only a simple integration; the complete result is presented here for possible adoptions as a reference flow for more complex problems. The general methods can often be considerably simplified for particular cases, such as shown in (B) and (C) where a combined use of the direct and inverse calculations can be made very effective and powerful. As a comparison, the integral iteration method has also been applied to (C). Finally, the circular arc problem is solved by using the integral iteration method, and the results compared with the available experiments.

All the numerical computations have been programmed and carried out on the IBM 7090 computer at California Institute of Technology. The errors involved in the computations, if explicitly verified, will be stated at the relevant place.

(A) *Symmetric wedge*

Consider the cavity flow past a symmetrical wedge of half vertex angle $\beta\pi$ as shown in figure 3(a). The limiting case of infinite cavity at $\sigma = 0$ is known as Bobyleff's problem; and the problem with arbitrary σ has been worked out with

various cavity models, e.g. with Riabouchinsky's model by Plesset & Shaffer (1948*a*, *b*), and Perry (1952), and with the wake model of Joukowsky and Roshko by Roshko (1954). The method given here is essentially not different from that of

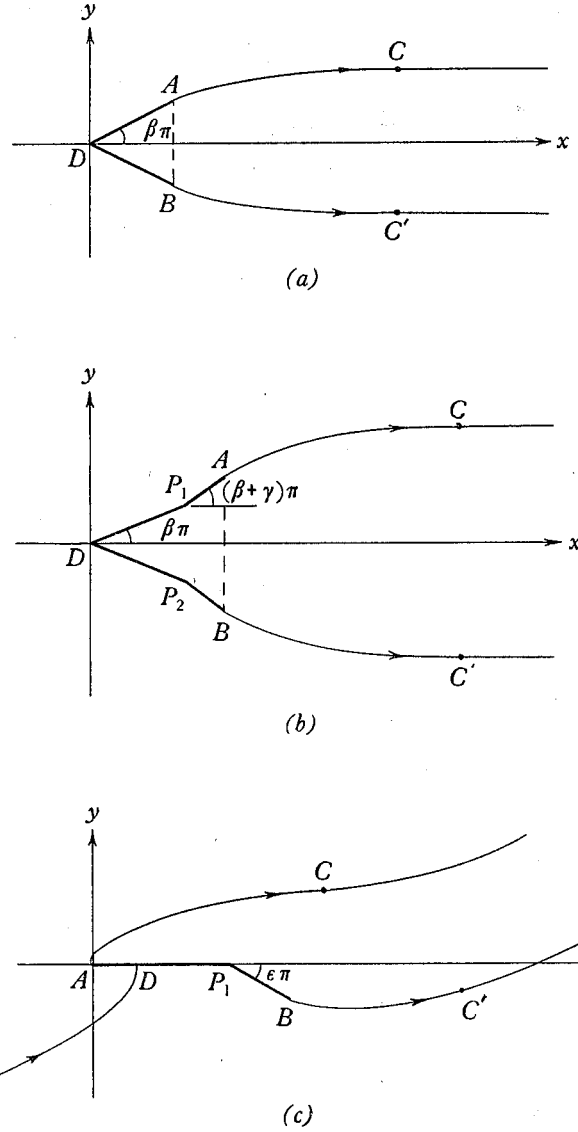

FIGURE 3. The co-ordinate systems and notations for specific cases.

Roshko who presented the numerical result for one case $\beta\pi = 45°$. We derive here the final result in a closed form and present numerical values in a wider range.

By symmetry it is obvious that

$$w = e^{i\pi\beta} t^{2\beta}. \tag{57}$$

At $z = \infty$, $w = U$, hence

$$t_0 = -iV, \quad V = U^{1/2\beta} = (1+\sigma)^{-1/4\beta}. \tag{58}$$

consequently, from (10)

$$f = At^2(t^2+V^2)^{-1}(t^2+V^{-2})^{-1}. \tag{59}$$

The physical plane is therefore

$$z = \int_0^t \frac{1}{w}\frac{df}{dt}dt = \frac{f(t)}{w(t)} + 2\beta e^{-i\pi\beta}\int_0^t t^{-(2\beta+1)}f(t)\,dt. \tag{60}$$

Let the length of one wedge face be l, then

$$\frac{l}{A} = \frac{V^2}{(1+V^2)^2} + 2\beta\int_0^1 \frac{t^{1-2\beta}dt}{(t^2+V^2)(t^2+V^{-2})} \equiv \Psi(\sigma;\beta). \tag{61}$$

From (48), (50) we readily deduce that $L = 0$ and

$$D = \pi\rho\beta A V^2(1-V^4)^{-1}(U^{-1}-U). \tag{62}$$

The drag coefficient based on the wedge base $b = 2l\sin\beta\pi$ is therefore

$$C_D(\sigma;\beta) = \frac{D}{\frac{1}{2}\rho U^2 b} = \frac{\pi\beta}{\sin\pi\beta}\left(\frac{V^{-2\beta}-V^{2\beta}}{V^{-2}-V^2}\right)\frac{(1+\sigma)}{\Psi(\sigma;\beta)}. \tag{63}$$

As $\sigma\to 0$, both U and V tend to unity, and we find the following asymptotic behaviour

$$C_D(\sigma;\beta) \sim \frac{4\pi\beta^2\csc\beta\pi}{1+8\beta\Psi_2(-\beta)}[1+\sigma+O(\sigma^2)], \tag{64a}$$

where

$$\Psi_n(\chi) = \frac{1}{2}\int_0^1 \frac{t^\chi}{(1+t)^n}dt, \tag{64b}$$

which can be expressed in terms of the logarithmic derivative of the Γ-function.

The above result for C_D is computed and shown in figure 4 versus the cavitation number σ for a number of the vertex angles $\beta\pi$. The present theory is found to be in good agreement with the experimental results of Waid (1957) and of Cox & Clayden (1958).

(B) *Two-step symmetric wedge*

Let us consider the cavity flow past a two-step symmetrical wedge with the inclination equal to $\beta\pi$ and $(\beta+\gamma)\pi$ on the first and second leg respectively ($0<\beta<1$, $0<(\beta+\gamma)<1$, see figure 3(*b*)), the flow being again symmetric about the x-axis and the imaginary t-axis. Let $t = \pm\tau$ correspond to the intermediate vertices, then

$$w = e^{i\pi\beta}t^{2\beta}(t^2-\tau^2)^\gamma(\tau^2t^2-1)^{-\gamma}. \tag{65}$$

At $z=\infty$, $w = U$ and $t_0 = -iV$, $0<V<1$, hence

$$\mu = (V^2+\tau^2)/(1+\tau^2V^2), \quad \mu \equiv (U/V^{2\beta})^{1/\gamma}. \tag{66a}$$

This equation may also be written

$$\tau^2 = (\mu-V^2)/(1-\mu V^2), \quad \text{or} \quad V^2 = (\mu-\tau^2)/(1-\mu\tau^2). \tag{66b}$$

Since $0<\tau^2<1$ and $0<V^2<1$, we deduce from (66*b*) that (i) $V^2<\mu<1$ and (ii) $\tau^2<\mu<1$. From (i) it immediately follows that

$$U^{1/2\beta} \lesseqgtr V \lesseqgtr U^{1/[2(\beta+\gamma)]} \quad \text{for} \quad \gamma \gtreqless 0. \tag{67}$$

(When γ is negative, $|\gamma|$ is taken to be small compared with β.) This inequality gives the range of V for prescribed $U = (1+\sigma)^{-\frac{1}{2}}$, and β, γ. The inequality (ii) then provides an upper bound for τ^2.

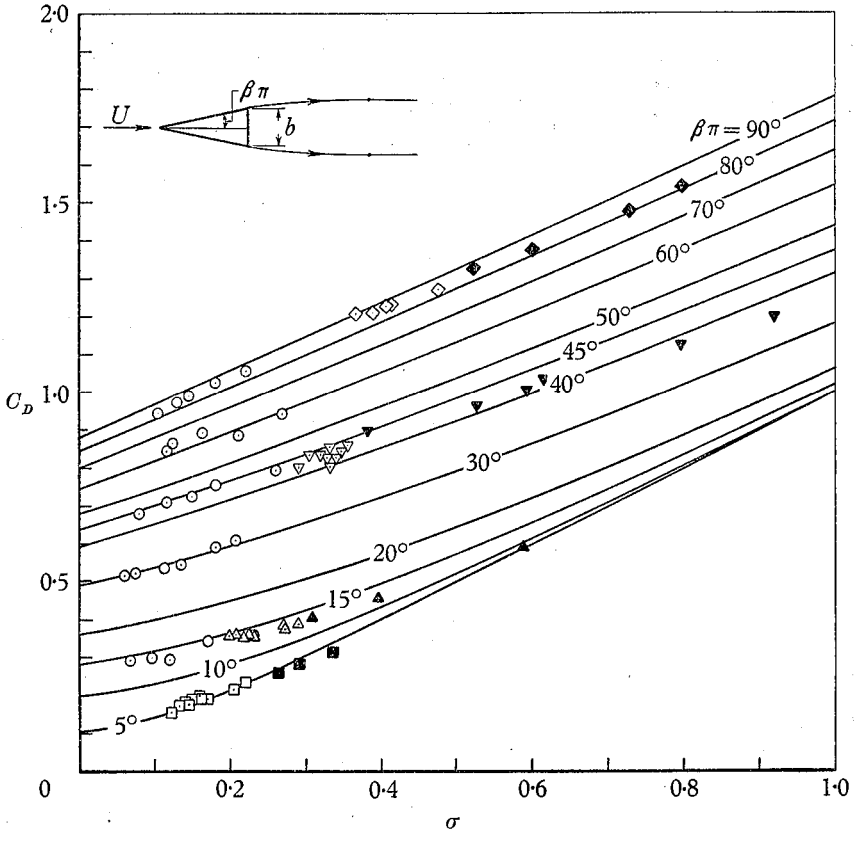

FIGURE 4. Variation of C_D with the cavitation number σ for symmetric wedges. Waid's data: $\beta\pi = 5°$, □; 15°, △; 45°, ▽; 90°, ◇; the solid symbols represent the corresponding data obtained when the cavity was filled with a mixture of water and gas bubbles. Cox & Clayden data: $\beta\pi = 15°, 30°, 45°, 60°, 90°$, all represented by ⊙.

The physical plane is given by

$$z = \int_0^t \frac{1}{w}\frac{df}{dt}\,dt = 2A\,e^{-i\pi\beta}\int_0^t \left(\frac{\tau^2t^2-1}{t^2-\tau^2}\right)^{\gamma} t^{1-2\beta}g(t)\,dt, \tag{68a}$$

where

$$g(t) = \frac{1}{2At}\frac{df}{dt} = \frac{(1-t^4)}{(t^2+V^2)^2\,(t^2+V^{-2})^2}. \tag{68b}$$

Let l_1 and l_2 be the lengths of the segment DP_1 and P_1A, then

$$\int_\tau^1 \left(\frac{1-\tau^2t^2}{t^2-\tau^2}\right)^{\gamma} t^{1-2\beta}g(t)\,dt = \frac{l_2}{l_1}\int_0^\tau \left(\frac{1-\tau^2t^2}{\tau^2-t^2}\right)^{\gamma} t^{1-2\beta}g(t)\,dt. \tag{69}$$

The width of the wedge base is

$$l_{AB} = 2[l_1 \sin \beta\pi + l_2 \sin(\beta+\gamma)\pi] = 4AF(\tau, V), \tag{70a}$$

$$F(\tau, V) = \left[\sin \beta\pi + \frac{l_2}{l_1}\sin(\beta+\gamma)\pi\right]\int_0^\tau \left(\frac{1-\tau^2 t^2}{\tau^2 - t^2}\right)^\gamma t^{1-2\beta} g(t)\, dt. \tag{70b}$$

For given $\beta, \gamma, \sigma, l_2/l_1$, the parameters V and τ can be determined from (66a) and (69). If use is made of (66b) in expressing $\tau = \tau(V)$, one can compute V directly from (69) as a function of $\beta, \gamma, \sigma, l_2/l_1$.

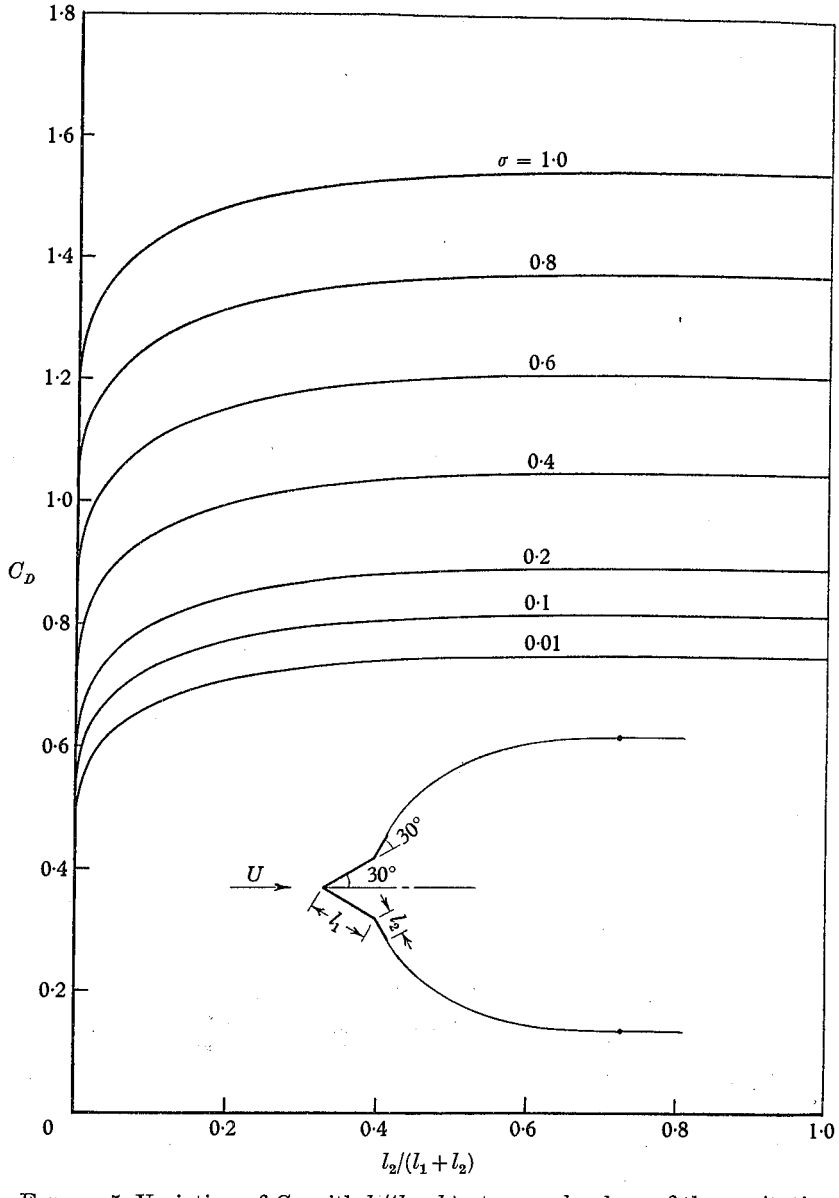

FIGURE 5. Variation of C_D with $l_2/(l_1+l_2)$ at several values of the cavitation number σ for the two-stepped wedge with $\beta\pi = \gamma\pi = 30°$.

Finally, application of (50) to this case gives $L = 0$, and

$$D = A\pi\rho \frac{U^{-1} - U}{V^{-2} - V^2} \left\{ \beta + \gamma \frac{(1-\tau^4)V^2}{(\tau^2+V^2)(1+\tau^2V^2)} \right\}. \tag{71}$$

Therefore the drag coefficient based on the base width is

$$C_D = \frac{D}{\frac{1}{2}\rho U^2 l_{AB}} = \frac{\pi}{2U^2} \frac{U^{-1} - U}{V^{-2} - V^2} \left\{ \beta + \gamma \frac{(1-\tau^4)V^2}{(\tau^2+V^2)(1+\tau^2V^2)} \right\} \frac{1}{F(\tau, V)}. \tag{72}$$

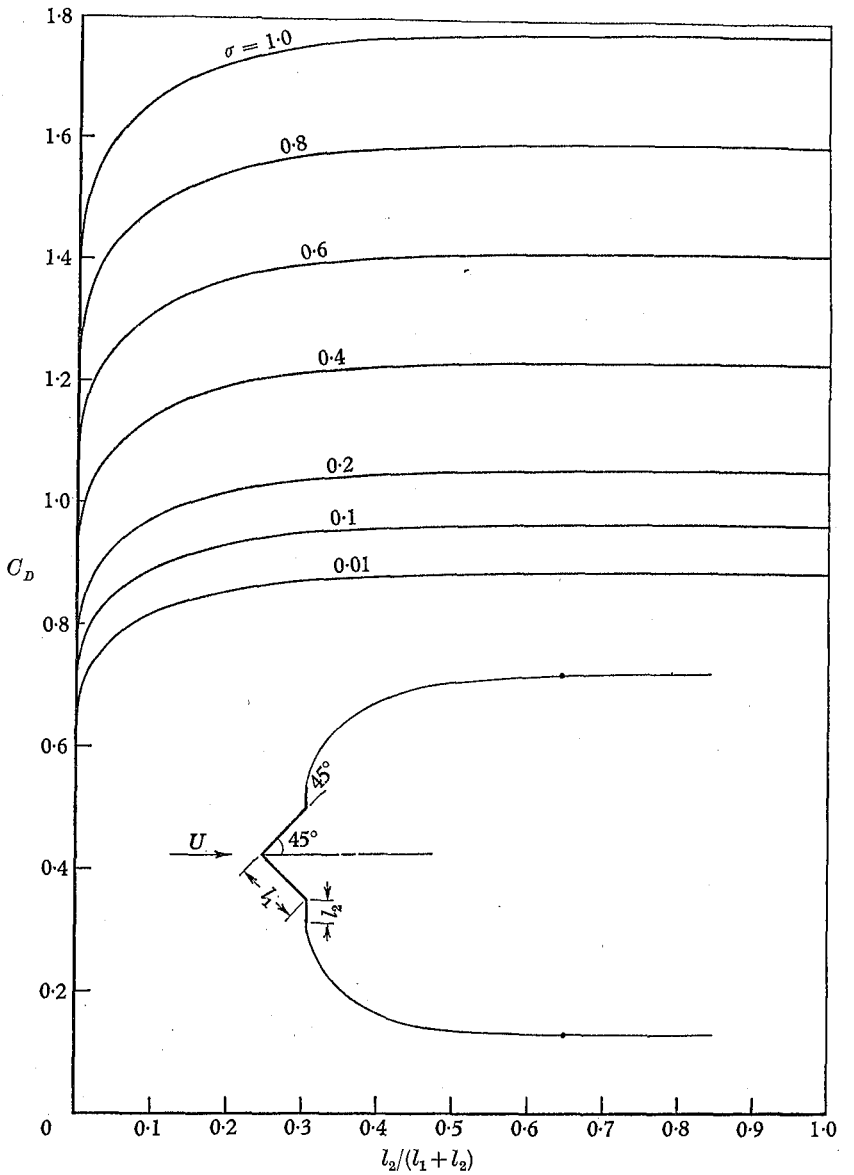

FIGURE 6. Variation of C_D with $l_2/(l_1+l_2)$ at several values of the cavitation number σ for the two-stepped wedge with $\beta\pi = \gamma\pi = 45°$.

A very straightforward scheme is adopted for the numerical computation in this case. For prescribed cavitation number σ (and hence U), a set of values of V are chosen within the region of (67), each of which then gives a fixed τ by (66b). The ratio l_2/l_1 can therefore be calculated from (69) as a function of $(U, V; \beta, \gamma)$

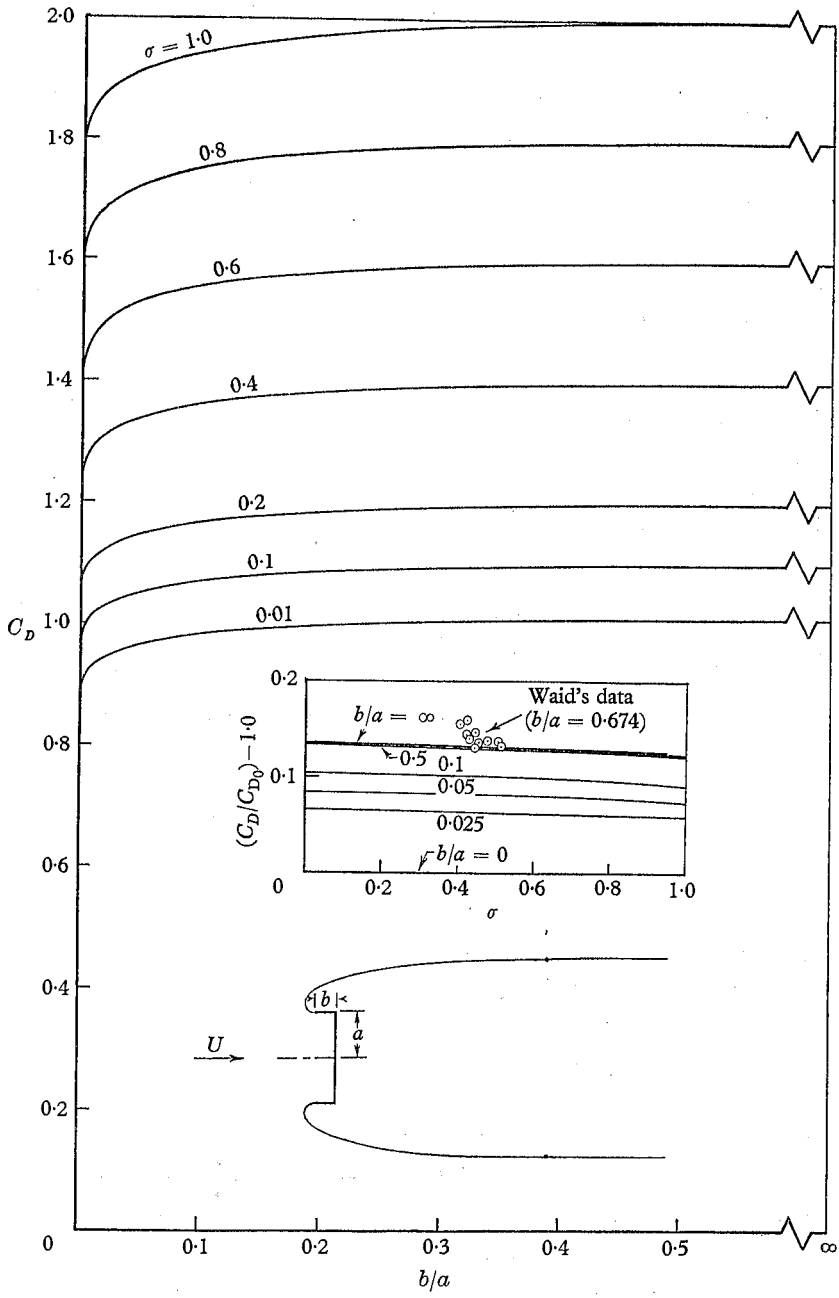

FIGURE 7. Variation of C_D with b/a at several values of σ for the rectangular cup (or with $\beta\pi = \gamma\pi = 90°$). Waid's data for $b/a = 0{\cdot}674$ are compared with the theory in the inserted figure.

from which readily follows the result for C_D given by (72). No further elaboration is needed here as the numerical work involved is rather simple. The drag coefficient C_D is shown versus $l_2/(l_1+l_2)$ with fixed values of σ in figures 5–7 for three special cases: $\beta\pi = \gamma\pi = 30°$, 45° and 90°. The last case has also been considered by Plesset & Perry (1954). The agreement between the present theory and the experiment of Waid (1957) may be regarded as good, as shown in an inserted cross-plot of figure 7. The result that Waid's data are all slightly higher than the theory for $b/a = \infty$ (for which case the flow is almost all stagnant inside the cup) may be due to the intrinsic feature of this flow model, or the wall effect which was not accounted for originally.

(C) *Flat plate with a flap*

As the simplest case of a polygonal obstacle in an asymmetrical flow we consider a flat plate AP_1 with an extended flap P_1B held at a flap angle $\epsilon\pi$ which will be taken positive here (see figure 3(*c*)). With the x-axis taken along AP_1, we have

$$w = t(t-\tau)^{\epsilon}(\tau t-1)^{-\epsilon}, \tag{73}$$

where $t = \tau$ is the image of the point P_1. At $z = \infty$, $w = U e^{-i\alpha}$, $t = t_0$, hence

$$t_0 = U e^{-i\alpha}(1-\tau t_0)^{\epsilon}(\tau - t_0)^{-\epsilon}. \tag{74}$$

From this equation it is readily seen that $U < |t_0| < 1$ (or see (13*a*)).

The physical plane is given by

$$z(t) = 2A\int_{-1}^{t}\left(\frac{\tau t-1}{t-\tau}\right)^{\epsilon} g(t;t_0)\,dt, \tag{75a}$$

where

$$g(t;t_0) = \frac{1}{2At}\frac{df}{dt} = \frac{(1-t^2)\,[1+t^2-\tfrac{1}{2}t(t_0+\bar{t}_0)\,(1+t_0^{-1}\bar{t}_0^{-1})]}{(t-t_0)^2\,(t-\bar{t}_0)^2\,(t-t_0^{-1})^2\,(t-\bar{t}_0^{-1})^2}. \tag{75b}$$

Let C and f_* be respectively the unflapped chord and the flap length. Then

$$\int_{-1}^{\tau}\left(\frac{1-\tau t}{\tau-t}\right)^{\epsilon} g(t;t_0)\,dt = \left(\frac{c}{f_*}-1\right)\int_{\tau}^{1}\left(\frac{1-\tau t}{t-\tau}\right)^{\epsilon} g(t;t_0)\,dt. \tag{76}$$

For convenience of computation, (76) can be written, by change of variables,

$$\int_0^1 \frac{g(t_1(u);t_0)}{u^{\epsilon}(1-\tau u)^2}\,du = \left(\frac{c}{f_*}-1\right)\int_0^1 \frac{g(t_2(u);t_0)}{u^{\epsilon}(1+\tau u)^2}\,du, \tag{77a}$$

where

$$t_1(u;\tau) = \frac{\tau-u}{1-\tau u}, \quad t_2(u;\tau) = \frac{\tau+u}{1+\tau u}. \tag{77b}$$

Finally, we derive from (50) for this case the lift and drag as

$$L = \frac{\pi\rho A(U^{-1}+U)\csc\alpha_0}{2(V^{-2}+V^2-2\cos 2\alpha_0)} \times\left\{\cos\alpha_0+\epsilon\frac{(1-\tau^2)\,[(1+\tau^2)V^2\cos\alpha_0-\tau V(1+V^2)\cos 2\alpha_0]}{(V^2+\tau^2-2V\tau\cos\alpha_0)\,(1+V^2\tau^2-2V\tau\cos\alpha_0)}\right\}, \tag{78a}$$

$$D = \frac{\pi\rho A(U^{-1}-U)/(1-V^2)}{2(V^{-2}+V^2-2\cos 2\alpha_0)} \times\left\{1+V^2+\epsilon\frac{(1-\tau^2)\,[(1+\tau^2)\,V^2(1+V^2)-2\tau V(1+V^4)\cos\alpha_0]}{(V^2+\tau^2-2V\tau\cos\alpha_0)\,(1+V^2\tau^2-2V\tau\cos\alpha_0)}\right\}, \tag{78b}$$

where $t_0 = V e^{-i\alpha_0}$.

Equations (74) and (76) are two equations for t_0 and τ which can be solved numerically for prescribed U, α, ϵ and f_*/c. In the numerical computation the following different schemes have been adopted. The very nature of this special problem permits a combined use of iteration and the inverse problem calculation. If we choose U, α, ϵ and τ as the independent parameters (which are a mixture of the physical and inverse parameters), then t_0 can be obtained from (74) by iteration†,

$$t_0^{(n)} = U e^{-i\alpha} \mathscr{F}(t_0^{(n-1)}; \tau, \epsilon) \quad \text{for} \quad n = 1, 2, \ldots, \tag{79a}$$

where

$$\mathscr{F}(t_0; \tau, \epsilon) = (1 - \tau t_0)^{\epsilon} (\tau - t_0)^{-\epsilon}, \tag{79b}$$

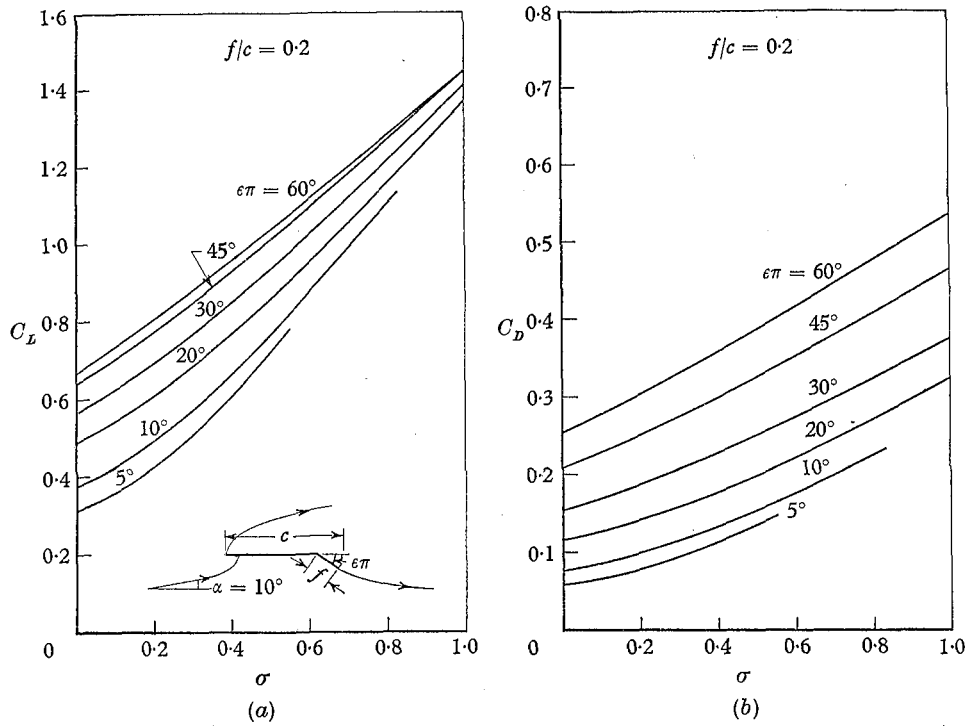

FIGURE 8. Variation of C_L and C_D with σ for a flat plate at incidence $\alpha = 10°$, with a flap of flap-chord ratio $f/c = 0{\cdot}2$ and held at flap deflexion $\epsilon\pi$.

and $t_0^{(0)}$ may be chosen to be $U e^{-i\alpha}$. This computation was programmed for an IBM 7090 electronic computer, and the iteration executed until an error of $|t_0^{(n)} - t_0^{(n-1)}| < 0{\cdot}0001$ is obtained. The convergence of this iteration is found to be very fast. With a series of τ chosen in $-1 < \tau < 1$, and with t_0 so determined, the remaining parameter f_*/c can then be determined readily from (76) or (77), and the lift and drag from (78). The accuracy of f_*/c and L, D depend on the $t_0^{(n)}$ used in the calculation, but otherwise their errors have not been explicitly determined by using two consecutive values of $t_0^{(n)}$. The numerical results of C_L and C_D (based on the chord c) are first plotted versus f_*/c (with the * deleted) for a set of values of σ and $\epsilon\pi$. From these figures the variation of C_L and C_D with σ can be obtained by cross-plotting, a typical case of $f/c = 0{\cdot}2$ being given in figure 8. The

† The iteration method is used here for the purpose of testing the rate of convergence.

special case of this problem with $\sigma = 0$ has recently been treated by Lin (1961) using Levi-Civita's method. The corresponding numerical results of these two cases are found to be in perfect agreement.

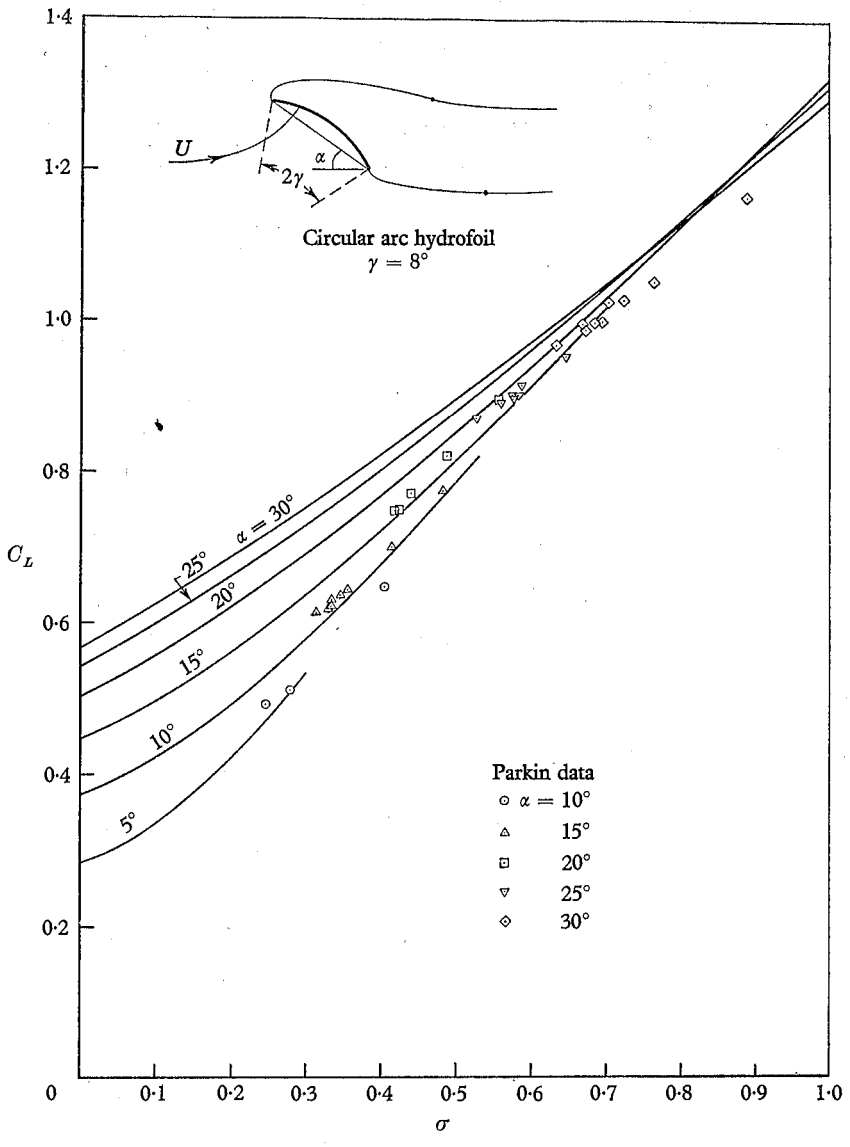

FIGURE 9. Variation of C_L with σ for a circular arc hydrofoil at incidence α.

It is easy to see that the above method (with τ_k chosen in order to calculate l_k) soon becomes impractically complicated with further increase in the number of polygonal faces. For the purpose of comparison, this problem has also been calculated by applying the general integral iteration method as described in § 5.1 which has been carried out on the IBM 7090 computer. It has been found that to obtain the same accuracy, the computer time for the integral iteration method is

considerably more than that for the method mentioned above. It is felt, however, that the integral iteration method will likely be more advantageous and time-saving when there are more than two consecutive flaps.

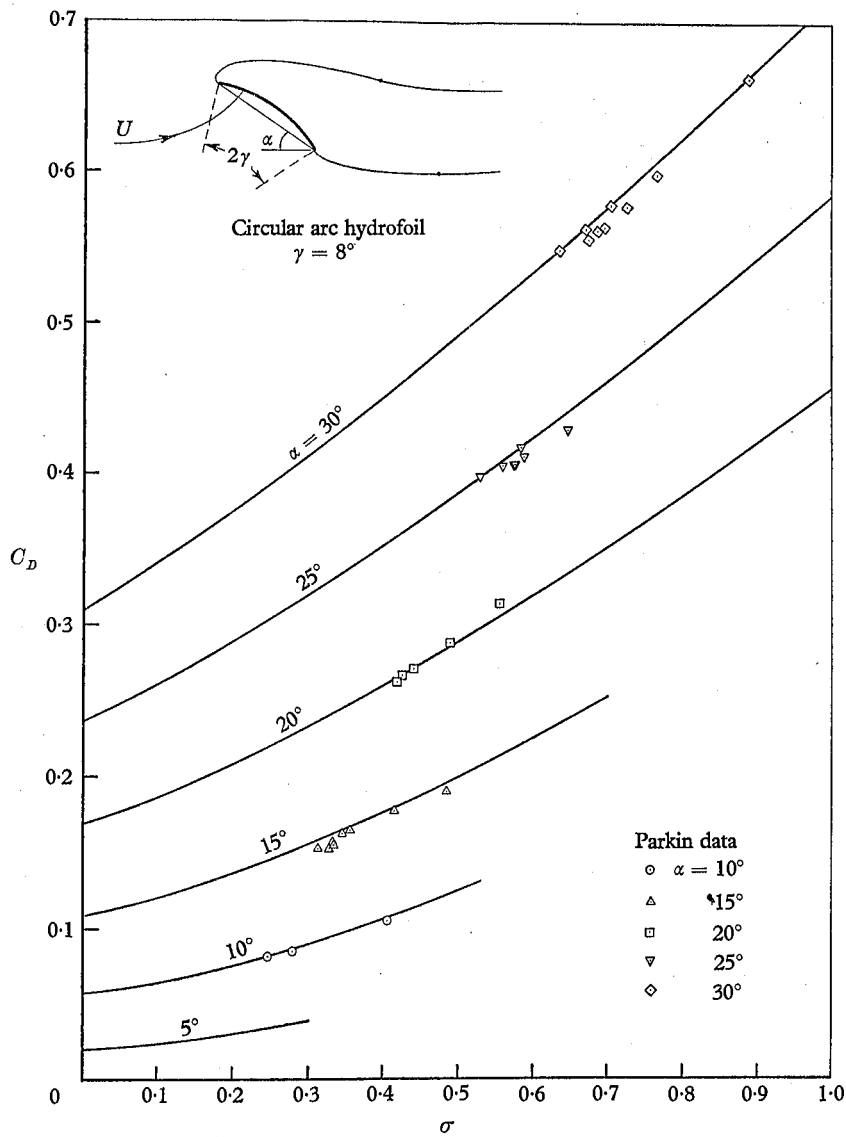

FIGURE 10. Variation of C_D with σ for a circular-arc hydrofoil at incidence α.

(D) *Circular-arc hydrofoil*

As an example of the general profile with continuously varying inclination, we consider the circular-arc hydrofoil with radius R and arc length $2\gamma R$ so that the arc angle is 2γ (see figure 9). The inclination β is a linear function of s

$$\beta(s) = \gamma - (s/R), \quad 0 < s < 2\gamma R. \tag{80}$$

The problem has previously been treated by Wu (1956*a*) adopting the wake model of Joukowsky and Roshko and using Levi-Civita's method in an approximate manner such that the series expansion is truncated and the boundary conditions on the inclination and curvature are satisfied only at the end points. The numerical work was carried out for $\gamma = 8°$ and the results compared with the experiments of Parkin (1956). The case of small γ has also been considered by Wu (1956*b*) as an example of the generalization of Tulin's linearized theory (1955) These two linear and non-linear theories have been compared for the case $\gamma = 8°$ (see Wu 1956*b*).

In order to compare the present cavity flow theory and the associated computational program with the previous non-linear theory (Wu 1956*a*), the numerical work of this problem has been carried out for $\gamma = 8°$, using the integral iteration method of § 5.1 on an IBM 7090 computer. In the computer program used in this case the conventional averaged-iteration process is employed. The iteration process is executed until the errors $|V^{(n)} - V^{(n-1)}|$ and $|\alpha_0^{(n)} - \alpha_0^{(n-1)}|$ are both less than 0·0001. The convergence of the iteration is considered to be very satisfactory. The resulting C_L and C_D (based on chord length $l_{AB} = 2R\sin\gamma$) are shown versus σ in figures 9 and 10, in which Parkin's experimental data (1956) are included for comparison. The C_D is found to be virtually identical with the previous approximate theory (Wu 1956*a*), whereas C_L of the present theory is slightly greater than the previous one for moderate values of σ.

This work was supported by the U.S. Office of Naval Research under Contract Nonr 220 (35).

REFERENCES

Birkhoff, G., Goldstine, H. H. & Zarantonello, E. H. 1954 *R.C. Semin. Mat. Torino*, **13**, 205–23.

Birkhoff, G. & Zarantonello, E. H. 1957 *Jets, Wakes and Cavities*. New York: Academic Press Inc.

Cox, A. & Clayden, W. 1958 Cavitating flow about a wedge at incidence. *J. Fluid Mech.* **3**, 615–37.

Gilbarg, D. 1960 *Jets and Cavities. Handbuch der Physik*, vol. IX, 311–445. Berlin: Springer-Verlag.

Leray, J. 1934 *C.R. Acad. Sci., Paris*, **199**, 1282.

Leray, J. 1935 Les problèmes de représentation conforme de Helmholtz. *Comment. math. helvet.* **8**, 149–80, 250–63.

Levi-Civita, T. 1907 Scie e leggi di resistenzia. *R.C. cir mat. Palermo*, **18**, 1–37.

Lin, J. D. 1961 A free streamline theory of flows about a flat plate with a flap at zero cavitation number. *Hydronautics, Inc., Rockville, Md, Tech. Rep.* no. 119–3.

Parkin, B. R. 1956 Experiments on circular-arc and flat-plate hydrofoils in non-cavitating and full cavity flows. *Calif. Inst. Tech. Hydro Lab. Rep.* no. 47–7 (see also 1958, *J. Ship Res.* **1**, 34–56).

Perry, B. 1952 The evaluation of integrals occurring in the cavity theory of Plesset and Shaffer. *Calif. Inst. Tech. Hydro. Lab. Rep.* no. 21–11.

Plesset, M. S. & Perry, B. 1954 *Mémoire sur la mecanique des fluids offerts á M. Dimitri Riabouchinsky*, pp. 251–61. Publ. Sci. Tech. Min. de l'Air, Paris.

Plesset, M. S. & Shaffer, P. A., Jr. 1948*a* Drag in cavity flow. *Rev. Mod. Phys.* **20**, 228–31.

Plesset, M. S. & Shaffer, P. A., Jr. 1948*b* Cavity drag in two and three dimensions. *J. App. Phys.* **19**, 934–39.

ROSHKO, A. 1954 A new hodograph for free streamline theory. *Nat. Adv. Comm. Aero., Wash., Tech note* no. 3168.

TULIN, M. P. 1955 Supercavitating flow past foils and struts. *Proc. Symp. on Cavitation in Hydrodynamics, N.P.L. Teddington.* London: Her Majesty's Stationery Office.

VILLAT, H. 1911 Sur la résistance des fluides. *Ann. sci. Éc. norm. sup., Paris*, **28**, 203–40.

VILLAT, H. 1914 Sur la validité des solutions de certains problemes d'hydrodynamique. *J. Math.* (6), **10**, 231–90.

WAID, R. 1957 Water tunnel investigations of two-dimensional cavities. *Calif. Inst. Tech. Hydro. Lab. Rep.* E-73.6.

WEINSTEIN, A. 1924 Ein hydrodynamischen Unitätssatz. *Math. Z.* **19**, 265–74.

WEINSTEIN, A. 1927 Sur le théorème d'existence des jets fluides. *R.C. R. Acad. dei Lincei*, p. 157.

WEINSTEIN, A. 1929 Zur theorie der Flüssigkeitsstrahlen. *Math. Z.* **31**, 424–33.

WU, T. Y. 1956*a*. A free streamline theory for two-dimensional fully cavitated hydrofoils. *J. Math. Phys.* **35**, 236–65.

WU, T. Y. 1956*b* A note on the linear and nonlinear theories for fully cavitated hydrofoils. *Calif. Inst. Tech. Hydro. Lab. Rep.* pp. 21–22.

WU, T. Y. 1962 A wake model for free streamline flow theory Part 1. Fully and partially developed wake flows and cavity flows past an oblique flat plate. *J. Fluid Mech.* **13**, 161–81.

Appendix

We present here an alternative derivation of the result $w = w(t)$ given by equation (23) in the text.

The boundary problem of the analytic function $\omega = i \log w = \theta + i\lambda$, which is defined in the upper half ζ-plane (see (7) and figure 1), may be expressed in terms of $\zeta = \xi + i\eta$ as

$$\begin{aligned} \operatorname{Im}\omega = \lambda = 0 \qquad & \text{for} \quad \eta = 0, \quad |\xi| < 1, \qquad (A\,1) \\ \operatorname{Re}\omega = \theta = \beta(s) \qquad & \text{for} \quad \eta = 0, \quad \xi > 1, \\ = \pi + \beta(s) \qquad & \text{for} \quad \eta = 0, \quad \xi < -1. \qquad (A\,2) \end{aligned}$$

Here, the function $\beta(s)$, defined by (21*b*), is assumed to be a known function of ξ. By virtue of (A 1) ω can be continued analytically into the lower half ζ-plane by Schwarz's principle of reflexion

$$\omega(\bar{\zeta}) = \overline{\omega(\zeta)}. \qquad (A\,3)$$

We shall adopt the notation $\omega^{\pm}(\xi) = \theta^{\pm}(\xi) + i\lambda^{\pm}(\xi)$ to signify the limit of ω as $\eta \to \pm 0$, respectively. Then from (A 3) it follows that $\theta^{+} = \theta^{-}$, $\lambda^{+} = -\lambda^{-}$. Thus, the original problem given by (A 1) and (A 2) may also be posed as the following Hilbert problem

$$\begin{aligned} \omega^{+} - \omega^{-} = 2i\lambda^{+} = 0 \qquad & \text{for} \quad |\xi| < 1; \qquad (A\,4) \\ \omega^{+} + \omega^{-} = 2\theta^{+} = 2\beta(s(\xi)) \qquad & \text{for} \quad \xi > 1, \\ = 2[\pi + \beta(s(\xi))] \qquad & \text{for} \quad \xi < -1. \qquad (A\,5) \end{aligned}$$

The general solution of this Hilbert problem can be written (see, for example, Muskhelishvili: Singular Integral Equations (1953), pp. 235–8)

$$\omega(\zeta) = \Omega(\zeta)\left\{\frac{1}{\pi}\int_{-\infty}^{-1} \frac{\pi + \beta(s(\xi))}{(\xi - \zeta)\sqrt{(\xi^2 - 1)}}\, d\xi - \frac{1}{\pi}\int_{1}^{\infty} \frac{\beta(s(\xi))\, d\xi}{(\xi - \zeta)\sqrt{(\xi^2 - 1)}} + \sum_{n=-\infty}^{\infty} C_n \zeta^n\right\}, \qquad (A\,6)$$

where $\Omega(\zeta) = i(\zeta^2-1)^{\frac{1}{2}}$, defined with a branch cut from $-\infty$ to -1 and from 1 to ∞ so that $\Omega \to i\zeta$ as $|\zeta| \to \infty$, $0 < \arg\zeta < \pi$, is a solution of the corresponding homogeneous Hilbert problem, and where C_n are arbitrary real coefficients. The solution can be determined uniquely only when the singular behaviour of ω is completely specified. For this problem we note that (i) $|\omega| < \infty$ along the free boundary, $\eta = 0$, $|\xi| < 1$, and (ii) $\omega \to O(\log\zeta)$ as $|\zeta| \to \infty$, the stagnation point. From these conditions it follows that $C_n = 0$ for all n. Consequently (A 6) reduces to the form (23) upon transformation to the t-plane by using (8).